Title

Cardiac Myocyte-Specific Excision of the β1 Integrin Gene Results in Myocardial Fibrosis and Cardiac Failure

Journal

Circulation Research, 90(4)

ISSN

0009-7330

Authors

Shai, Shaw-Yung
Harpf, Alice E
Babbitt, Christopher J
et al.

Publication Date

2002-03-08

DOI

10.1161/hh0402.105790

Peer reviewed

Cardiac Myocyte-Specific Excision of the β1 Integrin Gene Results in Myocardial Fibrosis and Cardiac Failure

Shaw-Yung Shai, Alice E. Harpf, Christopher J. Babbitt, Maria C. Jordan, Michael C. Fishbein, Ju Chen, Michelle Omura, Tarek A. Leil, K. David Becker, Meisheng Jiang, Desmond J. Smith, Simon R. Cherry, Joseph C. Loftus and Robert S. Ross

Circ Res. 2002;90:458-464; originally published online January 24, 2002;
doi: 10.1161/hh0402.105790
Circulation Research is published by the American Heart Association, 7272 Greenville Avenue, Dallas, TX 75231

Print ISSN: 0009-7330. Online ISSN: 1524-4571

Cardiac Myocyte–Specific Excision of the β1 Integrin Gene Results in Myocardial Fibrosis and Cardiac Failure

Shaw-Yung Shai, Alice E. Harpf, Christopher J. Babbitt, Maria C. Jordan, Michael C. Fishbein, Ju Chen, Michelle Omura, Tarek A. Leil, K. David Becker, Meisheng Jiang, Desmond J. Smith, Simon R. Cherry, Joseph C. Loftus, Robert S. Ross

Abstract—Integrins link the extracellular matrix to the cellular cytoskeleton and serve important roles in cell growth, differentiation, migration, and survival. Ablation of β1 integrin in all murine tissues results in peri-implantation embryonic lethality. To investigate the role of β1 integrin in the myocardium, we used Cre-LoxP technology to inactivate the β1 integrin gene exclusively in ventricular cardiac myocytes. Animals with homozygous ventricular myocyte β1 integrin gene excision were born in appropriate numbers and grew into adulthood. These animals had 18% of control levels of β1D integrin protein in the heart and displayed myocardial fibrosis. High-fidelity micromanometer-tipped catheterization of the intact 5-week-old β1 integrin knockout mice showed depressed left ventricular basal and dobutamine-stimulated contractility and relaxation (LV dP/dt_{max} and LV dP/dt_{min}) as compared with control groups (n=8 to 10 of each, $P<0.01$). Hemodynamic loading imposed by 7 days of transverse aortic constriction showed that the β1 integrin knockout mice were intolerant of this stress as they had 53% survival versus 88% in controls (n=15 each). By 6 months of age, mice with depressed ventricular expression of β1 integrin developed a dilated cardiomyopathy that was not evident in any control animals and had patchy decrease in glucose metabolism as determined by positron emission tomography. Myocyte membrane integrity as determined via Evan's blue dye staining was disrupted in the β1 integrin knockout mice. This model provides strong evidence for the importance of β1 integrin in cardiac form and function and indicates that integrins can be linked to development of cardiomyopathies. **(*Circ Res*. 2002;90:458-464.)**

Key Words: extracellular matrix ■ homologous recombination ■ Cre recombinase ■ heart ■ positron emission tomography

Integrins are a large family of heterodimeric cell surface receptors composed of α and β subunits. They function in cell–extracellular matrix (ECM) adhesion and cell-cell adhesion, and signal bidirectionally across the cell membrane.[1,2] Further, they serve as mechanotransducers, converting mechanical signals to biochemical ones.[3] This combination of properties allows integrins to play important roles in cell growth, differentiation, migration, and survival[4] and also makes them attractive candidates for essential roles in the developing and postnatal heart.

Our previous work has shown that β1 integrins are linked to the hypertrophic response of cultured ventricular myocytes and also that dominant-negative disruption of integrin function in transgenic mice resulted in cardiac fibrosis and abnormal cardiac function.[5–7] Ablation of β1 integrin expression in all murine tissues resulted in gastrulation defects and death by E5.5 of the 21-day gestation period.[8,9] Chimeric mice as well as embryoid bodies constructed from β1 integrin–null cells showed delayed development and differentiation of β1-deficient cells along the cardiac lineage, as well as abnormal sarcomerogenesis of these cardiac-like cells.[10] Although a few β1 integrin–null cells were detected in the myocardium of chimeric mice, cellular debris was always detected along with the null cells. These null cells were completely lost from the myocardium of the chimeric mouse heart by 6 months of age.

To more specifically evaluate the role of β1 integrin in the myocardium, we used a Cre-loxP gene targeting approach. Cre recombinase expression driven by the myosin light chain-2 ventricular (*MLC-2v*) promoter caused β1 integrin gene excision exclusively in ventricular cardiac myocytes.[11] Our results in these β1 knockout (β1KO) mice showed the following: (1) the β1 integrin gene was excised only in the heart; (2) β1D integrin protein in the myocardium was

Original received September 14, 2001; revision received January 16, 2002; accepted January 16, 2002.

From the Departments of Physiology (S.-Y.S., A.E.H., C.J.B., M.C.J., M.O., R.S.R.), Medicine (S.-Y.S., A.E.H., C.J.B., M.O., R.S.R.), Pathology (M.C.F.), and Anesthesia (M.J.); Cardiovascular Research and Mouse Physiology Laboratories (S.-Y.S., A.E.H., C.J.B., M.C.J., M.C.F., M.O., R.S.R.); and Department of Molecular and Medical Pharmacology and Crump Institute for Biological Imaging (T.A.L., D.J.S., S.R.C.), University of California–Los Angeles School of Medicine; Department of Medicine (J.C., K.D.B.), University of California–San Diego School of Medicine; and Mayo Clinic Scottsdale (J.C.L.), Scottsdale, Ariz. Present address for S.R.C. is Department of Biomedical Engineering, University of California–Davis.

Correspondence to Dr Robert S. Ross, Department of Physiology, University of California–Los Angeles School of Medicine, Center for the Health Sciences, Room 53-231, 10833 Le Conte Ave, Los Angeles, CA 90095-1751. E-mail ross@mednet.ucla.edu

Circulation Research **is available at http://www.circresaha.org** **DOI: 10.1161/hh0402.105790**

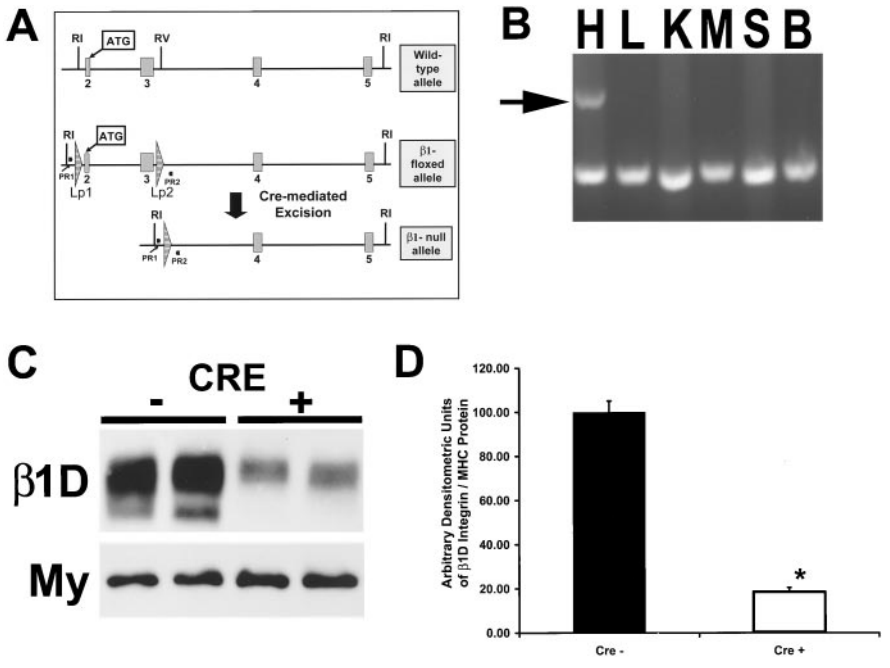

Figure 1. Generation of mice with cardiac-specific excision of β1 integrin gene. A, Partial maps of wild-type β1 integrin allele, β1 integrin–floxed allele, and β1 integrin–null allele. Exons and *loxP* sequences are indicated as rectangles and triangles, respectively. Translational start site (ATG) is located in the second exon as shown. Primers used for PCR confirmation of gene excision are designated as PR1 and PR2. Expression of Cre recombinase leads to deletion of the β1 integrin gene between LoxP1 and LoxP2, causing deletion of exons 2 and 3. RI indicates *Eco*RI; RV, *Eco*RV; and Lp, *loxP*. B, Ethidium bromide visualization of PCR products generated from genomic DNA derived from various tissues of the β1KO mouse. Duplex PCR was performed using 2 primer sets. One primer set as shown in panel A (PR1 and PR2) detected a 480-bp band only after excision of the portion of the β1 integrin gene between loxP site 1 (Lp1) and loxP site 2 (Lp2). Without excision, this PCR product would be 3300 bp. The 480-bp band (arrow) was only detected in heart. The lower 330-bp band was detected with a second primer set that amplified a portion of the Cre transgene, indicating that it was present in all tissues. Thus, Cre expression and subsequent Cre-mediated excision only occurred in heart. H indicates heart; L, lung; K, kidney; M, skeletal muscle; S, spleen; and B, brain. C, Western blot analysis of β1D integrin protein (top panel) as compared with sarcomeric myosin (My) heavy chain (bottom panel) in murine ventricle shows reduction of integrin protein only in mice expressing Cre recombinase (+). Data are representative of 3 independent experiments analyzing 9 samples in each group performed in 6-week-old animals. D, Densitometric analysis of Western blots showed that the normalized β1D integrin protein in hearts of Cre recombinase–expressing mice (Cre+) was reduced to <20% of the value of comparable samples obtained in mice that did not express Cre recombinase (Cre−) (n=9 each). Data are arbitrary densitometric units of β1 integrin protein normalized to sarcomeric myosin heavy chain protein. *$P<0.001$.

reduced to 18% of control levels; (3) β1KO mice developed postnatal cardiac fibrosis, had depressed cardiac function as determined by in vivo catheterization, and were intolerant of hemodynamic loading; (4) the hearts had abnormal myocardial glucose metabolism as determined by positron emission tomography (PET); (5) animals developed spontaneous heart failure by 6 months of age; and (6) animals showed abnormal myocyte membrane integrity as determined by Evan's blue dye (EBD) staining. These results demonstrate a critical function of β1 integrin in the postnatal myocardium and link this transmembrane protein to development of cardiomyopathy.

Materials and Methods

Antibodies and Reagents

The anti–β1D integrin antibody was created in our laboratory.[6] Anti-talin and anti-myosin (MF20) monoclonal antibodies were from Sigma and the Developmental Studies Hybridoma Bank, respectively. FITC- and rhodamine-labeled secondary antibodies were from Jackson ImmunoResearch Laboratories, Inc. Fluorescein-conjugated wheat germ agglutinin (F-WGA) was from Molecular Probes.

Construction of β1 Integrin–Floxed Mice and Ventricular-Specific Excision of the β1 Integrin Gene

Two clones 14 and 17 kb in length were isolated from a 129/SVJ mouse genomic library (Stratagene) and used for construction of the floxed β1 integrin gene–targeting vector, as shown in Figure 1A. R1 embryonic stem cells[12] were electroporated with the targeting vector, and successful homologous recombination was confirmed by Southern blot analysis using probes derived separately from intron 1 and exon 5 of the β1 integrin gene. (Data are shown in the expanded Materials and Methods section available online at http://www.circresaha.org.) The targeted embryonic stem cells were subjected to a second electroporation with pMC-Cre[13] and selected for resistance to 1-2′ deoxy-2′-fluoro-β-D-arabinofuranosyl-5′-iodouracil (FIAU [Moravek]). Colonies with Cre-mediated type II deletion were confirmed by polymerase chain reaction (PCR) analyses and injected into blastocysts to generate the targeted mice with a floxed β1 integrin gene. Mice with successful germline transmission of the targeted allele were identified and termed β1 integrin–floxed mice.

β1 integrin–floxed mice were mated to MLC2v-Cre mice[11,14] to generate animals with ventricular-specific β1 integrin gene inactivation ($\beta1^{flox/flox}$/$MLC2v^{Cre/+}$ or β1KO). Mice were analyzed in a 129SVJ/Black-Swiss background throughout the study, but results were confirmed in a 129/SVJ background. All animals were housed in an AALAC-approved facility.

Western Blot Analyses

Protein lysate preparation and Western blot were performed via standard methods.[7] Densitometry of samples (n=9 each group) was performed via use of either Alphaease (Alpha Innotech) or ImageQuant (Molecular Dynamics) software.

Hemodynamic Analysis, Transverse Aortic Constriction (TAC), and Echocardiography

Age-matched 5-week-old β1KO and control mice were used for both of these types of studies. Hemodynamic analyses at baseline and after dobutamine infusion were performed using in vivo catheterization with a micromanometer-tipped catheter.[7] For studies assessing survival after aortic constriction or sham operation, animals recovered from operative anesthesia, were returned to their cages, and were checked twice daily. Echocardiography was performed utilizing an Apogee CX echocardiographic machine (ATL Interspec).[15]

Micro–Positron Emission Tomography (MicroPET)

A microPET scanner developed at the UCLA Crump Institute for Biological Imaging, also available through Concorde Microsystems, was used to image the mice. Animals were anesthetized with 225 mg/kg avertin (2,2,2-tribromoethanol) (IP) and injected 20 minutes later with 200 to 233 mCi of [^{18}F]fluorodeoxyglucose (FDG). After an uptake period of 20 minutes, animals received additional anesthesia (ketamine, 100 mg/kg) and were imaged prone, in a long-axis orientation, with the microPET scanner. Scanner bed position was directly over the heart. Images were reconstructed using the maximum *a posteriori* reconstruction algorithm, which provides a resolution of ≈1.2 mm.[16]

Assay of Membrane Integrity

Six-month-old mice were injected intraperitoneally (50 μL/10 g body weight) with a 2% solution of EBD (Sigma) and euthanized 2 days after injection. Cryosections of myocardial tissue (5 to 7 μm) were examined under epifluorescent optics (as above) and viewed as a red image by using green activation (546 nm) and barrier (590 nm) filters, respectively.[17]

DNA Laddering and Terminal Deoxynucleotidyltransferase–Mediated dUTP Nick-End Labeling (TUNEL) Assays

DNA was extracted from 6-month-old β1KO and control mouse hearts and analyzed by agarose gel electrophoresis for nucleosomal DNA fragmentation. TUNEL assay was performed on heart cryosections by using Cardiotacs kit reagents (Trevigen), and visualization of TUNEL-positive cells was performed with FITC-ExtrAvidin (Sigma). Cardiomyocytes were detected with an anti-sarcomeric myosin antibody (MF20), and nuclei were localized by staining with DAPI (Sigma). Staining was visualized by immunofluorescent microscopy. TUNEL-positive cells were counted in multiple sections from each heart and recorded as TUNEL-positive myocytes/10 000 myocytes.

Statistics

The Student *t* test or ANOVA was used for analyses. $P<0.05$ was considered significant.

An expanded Materials and Methods section can be found in the online data supplement available at http://www.circresaha.org.

Results

Generation of Ventricular Muscle–Specific β1KO Mice

To generate mice that carry ventricular myocyte–restricted inactivation of the β1 integrin gene, we used a Cre-loxP strategy.[18] On the basis of previous successful ablation of the β1 integrin gene using a conventional knockout approach,[9] we constructed a floxed β1 integrin gene–targeting vector so that Cre recombinase–mediated excision would delete exon 2 (containing the translational start site) and exon 3, of the β1 gene (Figure 1A). This excision event would prevent expression of all β1 integrin isoforms since splice variation occurs downstream from these exons. We detected appropriate targeting and subsequent excision of the selectable markers in embryonic stem cells and produced gene-targeted mice via standard techniques.[19] Mice homozygous for a floxed β1 integrin gene were phenotypically normal and gave birth to litters of normal sizes.

To excise the β1 integrin gene specifically in cardiac ventricular myocytes, we bred the homozygous floxed β1 integrin mice to *MLC2v* Cre recombinase "knockin" mice that had been previously characterized.[11,14] Analysis of adult animals (ages 6 to 8 weeks) confirmed β1 integrin gene excision only in ventricular tissue derived from homozygous β1 *integrin flox×MLC2v-Cre* mice ($\beta1^{Flox/Flox}/MLC2v^{+/Cre}$) (Figure 1B). β1D integrin protein levels in the 6- to 8-week-old $\beta1^{Flox/Flox}/MLC2v^{+/Cre}$ mice were reduced to ≈20% of the control levels (18.6% ±1.9% versus controls, n=9 each, $P<0.001$), which were wild-type mice, homozygous floxed animals ($\beta1^{Flox/Flox}$) that had not been crossed with the *MLC2v-Cre* mice, or mice doubly heterozygous for the floxed β1 integrin allele and *MLC2v-Cre* ($\beta1^{Flox/+}/MLC2v^{+/Cre}$) (not shown) (Figures 1C and 1D). This amount of residual β1D integrin protein is in agreement with other studies using MLC2v-Cre–mediated excision.[11,20]

Conditional Gene Targeting of β1 Integrin Results in Cardiac Fibrosis and Ultrastructural Abnormalities in the Myocardium

We next evaluated the phenotype in the adult β1KO mice. Histological studies showed that patchy fibrosis developed in the ventricular wall of the $\beta1^{Flox/Flox}/MLC2v^{+/Cre}$ mice (Figures 2A and 2F). No comparable results were detected in age-, sex-, and strain-matched wild-type or $\beta1^{Flox/Flox}$ mice. In concert with identical reduction in β1 integrin protein expression, ventricular fibrosis was also detected when the $\beta1^{Flox/Flox}$ mice were crossed with a second cardiac-specific Cre mouse, in which the α-myosin heavy chain (*αMHC*) (5.5 kb) promoter drove Cre recombinase expression[21] (data not shown). Transmission electron microscopic analysis of affected areas of the β1KO myocardium showed focal dissolution of myofibrils and intercalated disks as well as mitochondrial swelling, with disruption and loss of cristae. No similar areas were detected in control animals (Figures 2G through 2H).

Temporal analysis showed that β1 integrin protein expression was reduced to 62.7±5.6% of control values (n=6) in the 2- to 3-week-old β1KO ventricle, to 23.4±5.7% of control values (n=3) in the 4-week-old ventricle, and to 18.6±1.9% of control values (n=9) by 6 to 8 weeks of age (Figure 2I). No histological abnormalities were detected in 3-week-old mouse hearts, whereas 22.1±6.8% fibrosis developed by age 6 to 8 weeks. These results suggested that β1 integrin is required for maintenance of cardiac myocyte and myocardial integrity.

β1 Integrin Protein Deficiency Leads to Abnormal Cardiac Function, Intolerance to Hemodynamic Loading, and Development of Heart Failure by 6 Months of Age

Cardiac function of the β1KO mice was evaluated with in vivo cardiac catheterization. Mice were analyzed at 5 weeks of age, when histological abnormalities were not extensive. Contractility and relaxation of the left ventricle in the $\beta1^{Flox/Flox}/MLC2v^{+/Cre}$ mice were significantly impaired as compared with any of the control groups (Figures 3A and 3D). Left ventricular end-diastolic pressure and heart rate did not vary significantly between groups. Because integrins can link transmission of force from the ECM to the cellular cytoskeleton, we challenged the β1KO mice by hemodynamic loading through TAC (Figure 3E). After 7 days of aortic

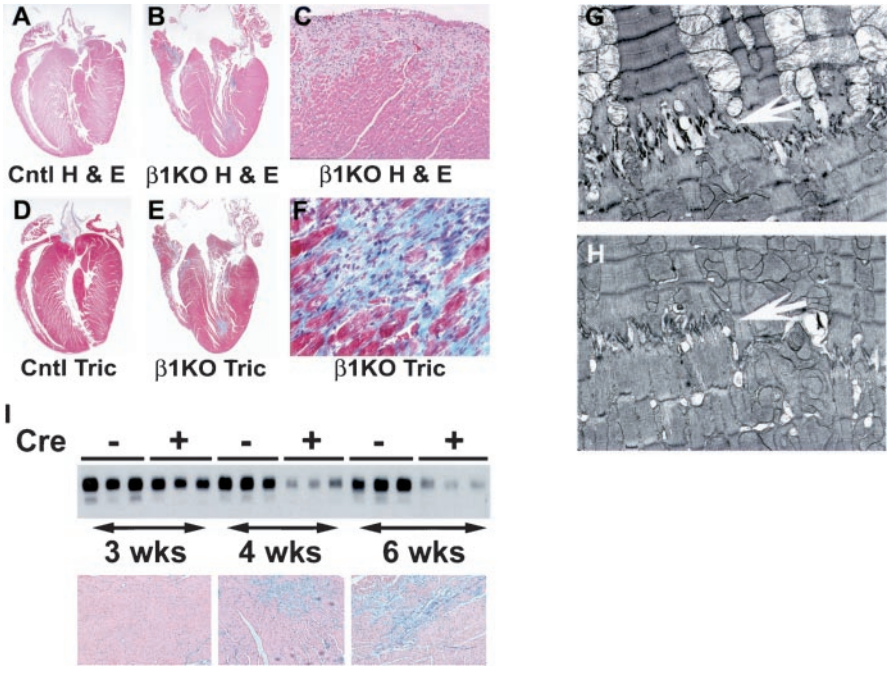

Figure 2. Abnormalities in mouse hearts from β1KO mice. A through F, Heart sections from 8-week-old control (Cntl; $\beta1^{Lox/Lox}$, no Cre) (A and D) and from β1KO mice (B, C, E, and F). A through C, Hematoxylin and eosin (H&E); D through F, Masson's trichrome (Tric). Patchy fibrosis was evident in β1KO ventricle (B and C), and collagen deposition was detected in trichrome-stained specimens (E and F). G and H, Electron micrographs of specimens from 4-month-old β1KO mouse heart (G) and control heart (H). Focal dissolution of myofibrils and intercalated disks (arrows), as well as mitochondrial swelling, was detected only in β1KO specimens but not in control animals. I, Temporal changes in β1 protein expression and development of fibrosis in β1KO mice. Top panel, Western blot analysis of β1D integrin expression in β1KO mice (Cre+) compared with control mice ($\beta1^{Lox/Lox}$ and $MLC2v^{+/+}$) (Cre−). Bottom panels show histology of heart sections from corresponding-age β1KO mice. Whereas no abnormalities were histologically visible in myocardium of 3-week-old β1KO mice, increasing fibrosis was detected with age to 22.1±6.8% at 6 to 8 weeks of age (n=5).

constriction, only 53% of the β1KO mice survived, whereas 88% survival was found in hemodynamically loaded $\beta1^{Flox/Flox}$/$MLC2v^{+/+}$ mice. No mortality occurred in sham-operated animals. These data suggested that β1 integrin is required for the murine ventricle to maintain normal function and that excessive hemodynamic demands are not tolerated by the β1 integrin–deficient ventricle.

When the β1 integrin–deficient mice reached ≈6 months of age, many of the animals showed clinical signs of congestive heart failure, including pleural effusions and liver congestion, and died spontaneously. Similar findings were evident in many β1KO postpartum female animals. Representative 6-month-old animals were examined pathologically, histologically, and echocardiographically. Histologically hearts showed dilation, replacement fibrosis, and even calcification within the ventricular wall and thrombi in enlarged atria (Figures 4A and 4B). M-mode echocardiography showed left ventricular chamber dilation, increased septal and free wall thicknesses, and depressed ventricular function (reduction in both percentage fractional shortening and velocity of circumferential fiber shortening) in β1KO animals as compared with controls (Figures 4C and 4D and the Table).

We evaluated cardiac metabolism in these β1-deficient animals by microPET (Figures 4E and 4F). β1KO mice displayed abnormal glucose metabolism in the ventricular tissue with patchy uptake of FDG throughout the ventricular myocardium and obvious dilation of the ventricular chamber in the β1KO mouse as compared with control littermates.

Distribution of Talin and Membrane Permeability Are Disrupted, but No Increase in Apoptosis Is Detected in β1KO Mouse Hearts

Because integrins link the ECM and cellular cytoskeleton and could stabilize cell membranes, we evaluated whether β1 integrin–deficient mice had altered membrane or actin binding protein characteristics. Talin binds directly to the β1 integrin cytoplasmic domain.[22] Immunostaining of heart tissue was performed with anti–β1D integrin and anti-talin antibodies (Figure 5A). Both β1 integrin and talin staining were uniformly visualized in the membranes of myocytes from control mice. In myocardial sections from the $\beta1^{Flox/Flox}$/$MLC2v^{+/Cre}$ mice, although residual β1D integrin protein was detected in some myocytes, its pattern even in those cells was non-uniform. This result was in agreement with our Western blot analyses (above). Normally even distribution of talin expression was also disrupted in the β1D integrin–deficient myocytes.

We performed EBD and WGA staining to detect membrane abnormalities in the myocardium. None of the cardiac myocytes in control mice were permeated by EBD (Figure 5B). Yet in multiple regions of the $\beta1^{Flox/Flox}$/$MLC2v^{+/Cre}$ mouse heart, strong red staining indicated that EBD-albumin complexes had entered these myocytes through permeant cell membranes. Similarly, imaging of control mouse myocardium with F-WGA demonstrated intact staining of myocyte cell membranes, whereas β1KO mouse heart sections showed disruption of cell membrane integrity.

Because disruption of cell adhesion can lead to apoptosis and decreased integrin expression can reduce cell adhesion, we evaluated for apoptosis in the β1KO mice. Ventricular DNA from our β1KO mice did not reveal DNA laddering (data not shown), nor were an increased number of TUNEL-positive myocytes detected in hearts of these mice (7±1.7 [β1KO] versus 9.2±1.9 [control] TUNEL-positive myocytes/10 000 myocytes; n=3 each group).

Discussion

Unlike the early embryonic lethality of the traditional β1KO mice,[9] our cardiac myocyte–specific β1KO mice survived to

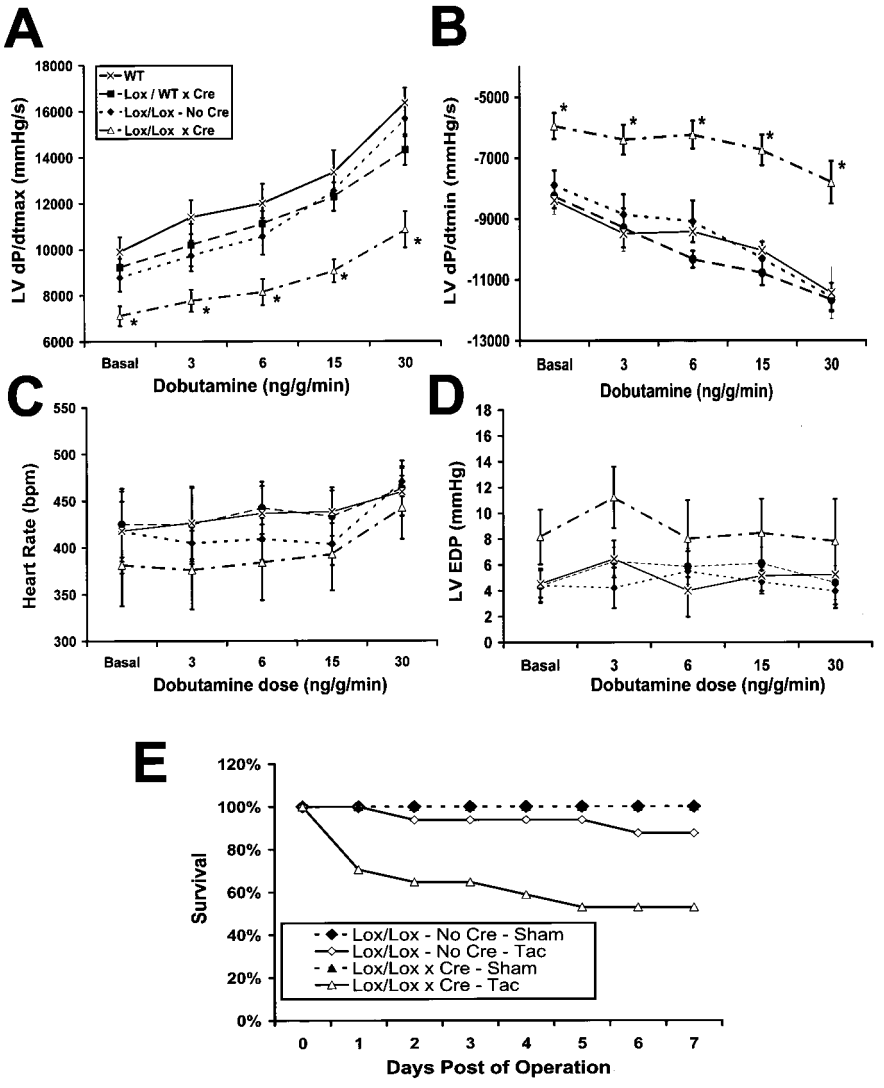

Figure 3. β1KO mice have abnormal cardiac function and intolerance to mechanical loading. A through D, In vivo hemodynamic analysis of β1KO and control mouse hearts. Cardiac catheterization was performed in intact, anesthetized mice of wild-type (WT, n=8), double-heterozygous ($\beta1^{Lox/+}$, $MLC2v^{Cre/+}$ [Lox/WT×Cre]; n=8), homozygous floxed ($\beta1^{Lox/Lox}$, $MLC2v^{+/+}$ [Lox/Lox–No Cre]; n=8), and β1KO ($\beta1^{Lox/Lox}$, $MLC2v^{Cre/+}$ [Lox/Lox×Cre]; n=10) using a micromanometer-tipped catheter. No significant difference was detected in either heart rate or left ventricular (LV) end-diastolic pressure (LVEDP), but LV dP/dt_{max} and LV dP/dt_{min} were both depressed basally and after dobutamine stimulation of β1KO mice compared with any other group. A, LV dP/dt_{max}, an index of cardiac contractility. B, LV dP/dt_{min}, an index of cardiac relaxation. C, Heart rate. D, LV end-diastolic pressure. Data are mean±SEM. A and B, *$P<0.01$. E, Survival analysis of β1KO mice after TAC. Shown are $\beta1^{Lox/Lox}$, $MLC2v^{+/+}$ (Lox/Lox–No Cre, sham operation); $\beta1^{Lox/Lox}$, $MLC2v^{+/+}$ (Lox/Lox–No Cre, TAC); $\beta1^{Lox/Lox}$, $MLC2v^{Cre/+}$ (Lox/Lox×Cre, sham operation); and $\beta1^{Lox/Lox}$, $MLC2v^{Cre/+}$, Lox/Lox×Cre, TAC). All groups, n=15. β1KO mice had 53% survival after hemodynamic loading compared with 88% of control animals.

adulthood likely because some β1 integrin protein was still present. Residual protein was present because of the incomplete nature of Cre-mediated excision effected by $MLC2v^{+/Cre}$ or *αMHC-Cre*, and is in agreement with previous published work that used these two Cre mice to effect excision of the connexin 43 and gp130 genes.[14,20] It is likely that further reduction of β1 integrin protein in the cardiac myocyte below a yet-unidentified "critical level" would result in abnormal cardiac development and embryonic lethality. This is currently being tested by mating our β1 integrin–floxed mice with animals that may express Cre in a more efficient manner in the cardiac myocyte.

In younger β1KO mice, there were few histological abnormalities, but in vivo catheterization detected abnormal cardiac function, and the mice were unable to tolerate hemodynamic loading. No evidence of morphometric hypertrophy or abnormal myocyte branching was detected in these animals. These findings demonstrate that β1 integrin is an important mechanotransducer in the cardiac myocyte as in other cell types.[23] Appropriate linkage of ECM and cytoskeleton through β1 integrins is essential for preservation of myocyte function.[3] When β1 integrin is reduced at the cell surface, this linkage is disrupted.

In older adult mice, we noted increased amounts of myocardial fibrosis and also found that the mice developed a dilated cardiomyopathy by 6 months of age. There was no consistent pattern of fibrosis within the ventricular wall, although some mice were found that displayed it in a subepicardial manner. Myocytes in the β1KO mice displayed membrane abnormalities as detected by positive EBD staining. We hypothesize that the ECM-cytoskeletal linkage, which in part occurs through integrins, is essential for maintenance of the cardiac myocyte, which undergoes continual hemodynamic demands in the beating myocardium. When the integrin is lost from the membrane, this important equilibrium is altered, myocyte integrity is compromised in a progressive manner, and myocyte necrosis occurs, leading ultimately to fibrotic replacement in the areas of the ventricle with myocyte loss. Cell adhesion has been suggested to be required for cell survival. More specifically, loss of adhesion to the ECM has been linked to cell apoptosis, a process termed anoikis.[24] It is for this reason that we tested for accelerated apoptosis in our KO mice, but no increase over control values was detected at the time assessed. It is likely that the cardiomyopathy resulted not only from replacement

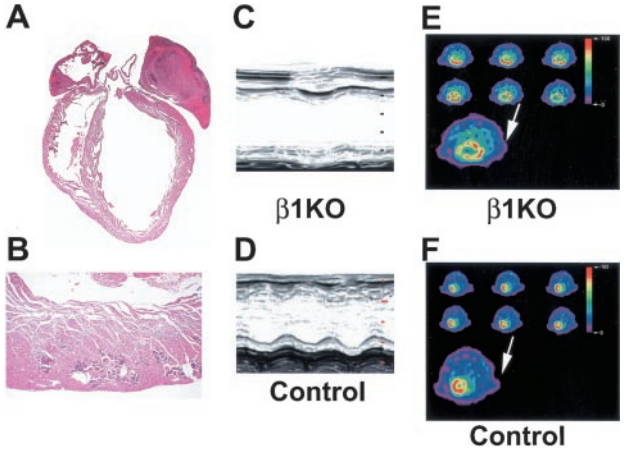

Figure 4. β1KO mice develop cardiac failure and have abnormal glucose metabolism by microPET. A and B, Histological analysis of representative 6-month-old β1KO mouse shows dilated chamber sizes, with clots in atria and fibrotic changes as well as calcium deposition in ventricular wall (as shown in higher-power view in panel B). C and D, Representative M-mode echocardiograms of β1KO (C) and age-matched control littermate (D) hearts show depressed left ventricular function, dilated right and left ventricular chambers, and thickened ventricular walls in β1KO heart. E and F, Results of microPET using FDG as a tracer of myocardial glucose utilization from a β1KO (E) and littermate control mouse (F). Highest levels of tracer uptake are depicted by red-orange, and lowest levels by purple, as indicated by color scale at top right of each panel. FDG uptake is decreased in a patchy manner in ventricle of β1KO hearts (E), which are also dilated compared with control animals (F). Arrows indicate enlarged view of denoted smaller images in panels E and F.

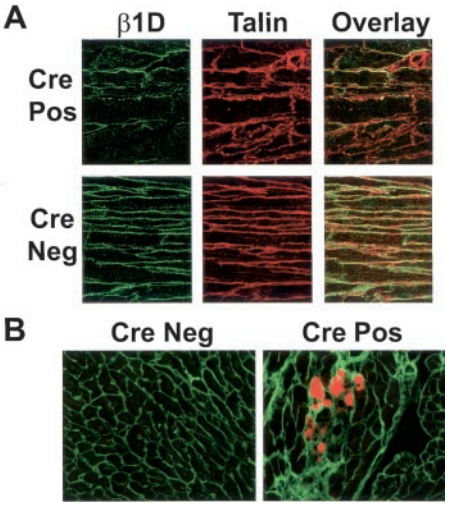

Figure 5. Abnormal integrin and talin distribution and membrane integrity are seen in β1KO hearts. A, Confocal microscopy with antibodies against β1D and talin shows abnormal cellular structure and organization in β1KO animals (Cre Pos) compared with age-matched littermate control samples (Cre Neg). β1KO animals showed varying cell sizes and irregular myocyte membrane staining compared with control mice. There was patchy loss of β1 integrin and disordered talin expression in β1KO animals. B, Representative images of EBD staining in β1KO animals (Cre Pos) compared with age-matched littermate control samples (Cre Neg). Sections were made from EBD-injected 6-month-old mouse hearts stained with F-WGA to identify cell membranes. Membrane staining is uniform in Cre-negative mouse with irregularities in the Cre-positive (β1KO) specimen. Control hearts did not show any red fluorescence (EBD/albumin complex penetration). On the contrary, Cre-positive (β1KO) mouse hearts displayed areas with red fluorescence, indicating that the membrane had become permeant to the EBD-albumin complex in the β1KO heart.

fibrosis of myocytes, but also from altered mechanotransduction of the β1 integrin–deficient myocytes. Deficiency of β1 integrin would lead to alterations in numerous αβ1 integrin heterodimer pairs, including α1β1. It is interesting to note that α1 integrin–null mice have increased expression of several matrix metalloproteinases (MMPs).[25] MMPs are linked to the remodeling that occurs during the development of cardiomyopathies, and thus it is possible that alterations in these molecules may also be present in our knockout mice. This is currently being investigated.

Echocardiographic Parameters in Anesthetized Mice

	Wild Type (n=5)	β1 Lox/Lox NO Cre (n=9)	β1 Lox/Lox Cre Positive (n=5)
LVEDD, mm	4.03±0.07	3.95±0.07	5.34±0.22*
LVESD, mm	2.87±0.09	2.69±0.05	4.89±0.20*
Sep th, mm	0.64±0.02	0.60±0.02	0.91±0.08*
PW th, mm	0.65±0.02	0.60±0.02	0.85±0.08*
FS, %	28.60±2.52	31.66±1.20	8.44±1.53*
Vcfc, circ/s	6.51±0.63	6.75±0.29	2.25±0.62*

Values are mean±SEM. n indicates number of mice; LVEDD, left ventricular end-diastolic dimension; LVESD, left ventricular end-systolic dimension; Sep th, ventricular septal thickness; PW th, left ventricular posterior wall thickness; FS, fractional shortening; Vcfc, velocity of circumferential fiber shortening; and circ/s, circumferences per second.

*$P<0.001$ by ANOVA with Bonferroni posttest.

Parallels can be drawn between these integrin KO mice and changes that occur in muscular dystrophy. Like integrins, the dystrophin-glycoprotein complex also links the ECM and intracellular cytoskeleton. With loss of components of this complex, alteration in membrane permeability is seen and cardiomyopathy can result.[17,26] Although integrin mutations have been linked to skeletal muscle dystrophies in animal models and in humans, they have not been previously linked to cardiomyopathy.[27–31] Further, it is interesting to note that in muscles from *mdx* mice and patients with Duchenne and Becker dystrophies, increased expression of α7 integrin transcript and protein were detected. Thus, integrins may compensate for absence of components of the dystrophin-dystroglycan complex. This has been recently shown in a mouse model of muscular dystrophy in which overexpression of α7 integrin improved many of the clinical features of the disease.[32] Further, α7 integrin–null mice develop progressive skeletal muscular dystrophy, although cardiac function has not been studied in this model. In contrast to integrin upregulation in the absence of dystrophin-dystroglycan complex proteins, no compensatory change in dystrophin, dystroglycan, or α-sarcoglycan was detected in the α7 integrin–null background.[31] Thus, this model gives further credence to the importance of integrins as an indispensable linkage between muscle fiber (and perhaps cardiac myocytes) and the ECM.

This linkage appears independent of the dystrophin-dystroglycan complex–mediated interaction of the cytoskeleton with the muscle basement membrane. Thus, there are clearly distinct functions of these two types of transmembrane proteins. This is emphasized by recent data that found that dystroglycan was necessary for initial binding of laminin to the cell surface, whereas β1 integrin was subsequently required for laminin matrix assembly after the binding.[33] We would suggest that integrin mutations could ultimately be detected in a subset of cardiomyopathy patients.

The strategy we used to target exons 2 and 3 of the β1 integrin gene reduces all isoforms of this protein. In the heart, the dominant postnatal isoform of β1 integrin is β1D.[6] Previous work has shown that β1D cannot substitute for β1A integrin in all organs; doing so leads to fetal lethality with multiple developmental defects.[34] Conversely, full ablation of β1D was suggested to lead to a "mild" cardiac phenotype represented by increased expression of atrial natriuretic factor in the β1D-null adult mouse ventricle.[34] Our results provide more comprehensive analysis of the cardiac function in β1 integrin–deficient mice but cannot discriminate between absence of β1A or β1D as the prime cause of the resultant phenotype. Studies are currently underway to test the ability of cardiac-specific expression of β1A or β1D, to alter the β1KO phenotype.

In summary, we have produced a murine model with cardiac-specific β1 integrin deficiency resulting in abnormal cardiac function and cardiomyopathy. This animal model will be useful for determination of integrin function in the myocardium and other tissues.

Acknowledgments

This work was supported by NIH Grants HL57872 (to R.S.R.) and HL67938 (to J.C.L.) and by the UCLA Laubisch Cardiovascular Research Fund. We thank Dr Lutz Birnbaumer for assistance in embryonic stem cell work, Dr Joy Frank and Tony Mottino for assistance with electron microscopy, Dr Matthew Schibler for confocal microscopy support, and Dr Robb MacLellan for reagents and critical advice.

References

1. Calderwood DA, Shattil SJ, Ginsberg MH. Integrins and actin filaments: reciprocal regulation of cell adhesion and signaling. *J Biol Chem*. 2000; 275:22607–22610.
2. Hynes RO. Integrins: versatility, modulation, and signaling in cell adhesion. *Cell*. 1992;69:11–25.
3. Ingber DE. Cellular basis of mechanotransduction. *Biol Bull*. 1998;194:323–325.
4. Gumbiner BM. Cell adhesion: the molecular basis of tissue architecture and morphogenesis. *Cell*. 1996;84:345–357.
5. Ross RS, Pham C, Shai SY, Goldhaber JI, Fenczik C, Glembotski CC, Ginsberg MH, Loftus JC. β_1 integrins participate in the hypertrophic response of rat ventricular myocytes. *Circ Res*. 1998;82:1160–1172.
6. Pham CG, Harpf AE, Keller RS, Vu HT, Shai SY, Loftus JC, Ross RS. Striated muscle-specific β(1D)-integrin and FAK are involved in cardiac myocyte hypertrophic response pathway. *Am J Physiol Heart Circ Physiol*. 2000;279:H2916–H2926.
7. Keller RS, Shai SY, Babbitt CJ, Pham CG, Solaro RJ, Valencik ML, Loftus JC, Ross RS. Disruption of integrin function in the murine myocardium leads to perinatal lethality, fibrosis, and abnormal cardiac performance. *Am J Pathol*. 2001;158:1079–1090.
8. Stephens LE, Sutherland AE, Klimanskaya IV, Andrieux A, Meneses J, Pedersen RA, Damsky CH. Deletion of β_1 integrins in mice results in inner cell mass failure and peri-implantation lethality. *Genes Dev*. 1995;9:1883–1895.
9. Fassler R, Meyer M. Consequences of lack of β_1 integrin gene expression in mice. *Genes Dev*. 1995;9:1896–1908.
10. Fassler R, Rohwedel J, Maltsev V, Bloch W, Lentini S, Guan K, Gullberg D, Hescheler J, Addicks K, Wobus AM. Differentiation and integrity of cardiac muscle cells are impaired in the absence of β_1 integrin. *J Cell Sci*. 1996;109(pt 13):2989–2999.
11. Chen J, Kubalak SW, Chien KR. Ventricular muscle-restricted targeting of the RXRα gene reveals a non-cell-autonomous requirement in cardiac chamber morphogenesis. *Development*. 1998;125:1943–1949.
12. Joyner AL. *Gene Targeting: A Practical Approach*. Oxford, UK: IRL Press at Oxford University Press; 1993.
13. Gu H, Zou YR, Rajewsky K. Independent control of immunoglobulin switch recombination at individual switch regions evidenced through Cre-loxP-mediated gene targeting. *Cell*. 1993;73:1155–1164.
14. Hirota H, Chen J, Betz UA, Rajewsky K, Gu Y, Ross J Jr, Muller W, Chien KR. Loss of a gp130 cardiac muscle cell survival pathway is a critical event in the onset of heart failure during biomechanical stress. *Cell*. 1999;97:189–198.
15. Gottshall KR, Hunter JJ, Tanaka N, Dalton N, Becker KD, Ross JJ, Chien KR. Ras-dependent pathways induce obstructive hypertrophy in echo-selected transgenic mice. *Proc Natl Acad Sci U S A*. 1997;94:4710–4715.
16. Qi J, Leahy RM, Cherry SR, Chatziioannou A, Farquhar TH. High-resolution 3D Bayesian image reconstruction using the microPET small-animal scanner. *Phys Med Biol*. 1998;43:1001–1013.
17. Ikeda Y, Martone M, Gu Y, Hoshijima M, Thor A, Oh SS, Peterson KL, Ross J Jr. Altered membrane proteins and permeability correlate with cardiac dysfunction in cardiomyopathic hamsters. *Am J Physiol Heart Circ Physiol*. 2000;278:H1362–H1370.
18. Marth JD. Recent advances in gene mutagenesis by site-directed recombination. *J Clin Invest*. 1996;97:1999–2002.
19. Hogan B, Costantini F, Lacy E. *Manipulating the Mouse Embryo*. Plainview, NY: Cold Spring Harbor Press; 1986.
20. Gutstein DE, Morley GE, Tamaddon H, Vaidya D, Schneider MD, Chen J, Chien KR, Stuhlmann H, Fishman GI. Conduction slowing and sudden arrhythmic death in mice with cardiac-restricted inactivation of connexin43. *Circ Res*. 2001;88:333–339.
21. Agah R, Frenkel PA, French BA, Michael LH, Overbeek PA, Schneider MD. Gene recombination in postmitotic cells: targeted expression of Cre recombinase provokes cardiac-restricted, site-specific rearrangement in adult ventricular muscle in vivo. *J Clin Invest*. 1997;100:169–179.
22. Pfaff M, Liu S, Erle DJ, Ginsberg MH. Integrin β cytoplasmic domains differentially bind to cytoskeletal proteins. *J Biol Chem*. 1998;273:6104–6109.
23. Gudi SR, Lee AA, Clark CB, Frangos JA. Equibiaxial strain and strain rate stimulate early activation of G proteins in cardiac fibroblasts. *Am J Physiol*. 1998;274:C1424–C1428.
24. Frisch SM, Ruoslahti E. Integrins and anoikis. *Curr Opin Cell Biol*. 1997;9:701–706.
25. Pozzi A, Moberg PE, Miles LA, Wagner S, Soloway P, Gardner HA. Elevated matrix metalloprotease and angiostatin levels in integrin α_1 knockout mice cause reduced tumor vascularization. *Proc Natl Acad Sci U S A*. 2000;97:2202–2207.
26. Tsubata S, Bowles KR, Vatta M, Zintz C, Titus J, Muhonen L, Bowles NE, Towbin JA. Mutations in the human δ-sarcoglycan gene in familial and sporadic dilated cardiomyopathy. *J Clin Invest*. 2000;106:655–662.
27. Burkin DJ, Kaufman SJ. The $\alpha_7\beta_1$ integrin in muscle development and disease. *Cell Tissue Res*. 1999;296:183–190.
28. Cohn RD, Mayer U, Saher G, Herrmann R, van der FA, Sonnenberg A, Sorokin L, Voit T. Secondary reduction of α_{7B} integrin in laminin α_2 deficient congenital muscular dystrophy supports an additional transmembrane link in skeletal muscle. *J Neurol Sci*. 1999;163:140–152.
29. Vachon PH, Xu H, Liu L, Loechel F, Hayashi Y, Arahata K, Reed JC, Wewer UM, Engvall E. Integrins ($\alpha_7\beta_1$) in muscle function and survival: disrupted expression in merosin-deficient congenital muscular dystrophy. *J Clin Invest*. 1997;100:1870–1881.
30. Hayashi YK, Chou FL, Engvall E, Ogawa M, Matsuda C, Hirabayashi S, Yokochi K, Ziober BL, Kramer RH, Kaufman SJ, Ozawa E, Goto Y, Nonaka I, Tsukahara T, Wang JZ, Hoffman EP, Arahata K. Mutations in the integrin α_7 gene cause congenital myopathy. *Nat Genet*. 1998;19:94–97.
31. Mayer U, Saher G, Fassler R, Bornemann A, Echtermeyer F, von der MH, Miosge N, Poschl E, von der MK. Absence of integrin α_7 causes a novel form of muscular dystrophy. *Nat Genet*. 1997;17:318–323.
32. Burkin DJ, Wallace GQ, Nicol KJ, Kaufman DJ, Kaufman SJ. Enhanced expression of the $\alpha_7\beta_1$ integrin reduces muscular dystrophy and restores viability in dystrophic mice. *J Cell Biol*. 2001;152:1207–1218.
33. Henry MD, Satz JS, Brakebusch C, Costell M, Gustafsson E, Fassler R, Campbell KP. Distinct roles for dystroglycan, β_1 integrin and perlecan in cell surface laminin organization. *J Cell Sci*. 2001;114:1137–1144.
34. Baudoin C, Goumans MJ, Mummery C, Sonnenberg A. Knockout and knockin of the β_1 exon D define distinct roles for integrin splice variants in heart function and embryonic development. *Genes Dev*. 1998;12:1202–1216.

Supplementary Methods

Construction of β1 integrin floxed mice and ventricular-specific excision of the β1 integrin gene.

A 129/SVJ mouse genomic library in Lambda FIX II (Stratgene) was screened with a combination of two 45-bp oligonucleotide probes coding for the region of the β1 integrin gene overlapping its known translational start site (Primer A = 5'-AAGAAGGAATGCCTACTTCTGCACGATGTGATGATTTAGAAGCTT-3', bases 163-207 and Primer B = 5'-TGTCACTTGGCTGGCAACCCTTCTTTTTCAAAGCTTCTAAATCAT-3', bases 237-193 of Genbank Accession # X15202, Mouse mRNA for fibronectin receptor beta-chain VLA5-homolog, respectively.) Two clones, 14 and 17 kb in lengths were identified and subcloned into the unique NotI site of pBS II SK (Stratagene), yielding clones pBeta1-14 and pBeta1-17. Clones were extensively mapped and sequenced for further preparation of the final targeting construct. To assemble the targeting vector, native pBS II SK was first modified to contain a BstEII site by cloning a BstEII linker between the BamHI and XbaI sites of the parent plasmid. Then, this modified pBS II SK vector, was used in combination with components of the plasmid pFlox[1] to sequentially clone and produce the targeting construct vector.

(Supplementary figure 1, panel B)

The β1 integrin targeting vector was linearized with NotI prior to electroporation of R1 ES cells[2]. Following growth and selection, DNA derived from prospectively targeted ES cells was screened by Southern blotting using a probe from the 5th exon of the β1 integrin gene (**as**

diagrammed in Supplementary figure 1, panel A) which would be located outside the region of the targeting construct. Southern blotting of EcoRI cut genomic ES cell DNA from potentially targeted ES cells with this probe detected a wild-type 12.5 kb band, and in the clones generated from appropriate targeting of the β1 integrin gene locus, a unique 9.4 kb band. **(Supplementary figure 1, panel A and C as well as Supplementary figure 2, panel A).** Similarly, Southern blotting of BamHI cut ES cell genomic DNA probed with an intron 1 probe **(diagrammed in Supplementary figure 1, panel A)** detected a wild-type 10.9 kb band and a unique 5.1 kb band in the appropriately targeted ES cell clones. **(Supplementary figure 2, panel B).** Clones with similar intensity of the unique and wild-type bands were chosen for further use.

The targeted ES cells were subjected to a second electroporation with pMC-Cre [3] and selected for deletion of the Neo-TK selectable marker in 1-2' deoxy-2'-fluro-β-D-arabinofuranosyl-5'-iodouracil (FIAU, Moravek). Cre-mediated Type II deletion was examined by polymerase chain reaction (PCR) analyses using unique primers **PR2**: 5'-AAGACAGGGTTTCTCTGT GTAG-3' and **PR3**: 5'- TATGAGGCTCCTTGATTGGTCA-3', as diagrammed in **Supplementary figure 2, panel C.** Representative PCR results are shown in **Supplementary figure 2, panel D** where use of primers 2 and 3 generated a 167 bp band from the wild-type β1 integrin allele and a 245 bp band in clones from which the selectable marker had been excised. Southern blotting was used to confirm this result (data not shown). Clones with appropriate type II deletion were expanded for injection into the blastocysts.

Western blot analyses.

Hearts were dissected, rinsed in PBS, and immediately homogenized on ice in 1 ml ice-cold RIPA buffer (158 mM NaCl, 10 mM Tris-HCl pH 7.2, 1 mM EGTA, 1 mM orthovanadate, 1% triton-X100, 1% Na deoxycholate, 0.1% SDS, 100 μM leupeptin, 5 IU/ml aprotinin, 10

μg/ml soybean trypsin inhibitor, 10 mM benzamidine and 1 mM PMSF) and incubated for 10 min on ice. Lysates were clarified by centrifugation (16,000g, 15 min, at 4°C). Protein content of the lysate was determined using the BCA protein assay (Biorad Laboratories). For immunoblotting, equal amounts of protein (2-10 μg) were electrophoresed on an 8-16% gradient SDS-PAGE gel and transferred onto Immobilon-P (Millipore Corporation). Signals were detected using enhanced chemiluminescence (ECL) (Amersham Pharmacia Biotech). Densitometry of samples (n=6-9 each group) was performed via use of either Alphaease (Alpha Innotech) or ImageQuant (Molecular Dynamics) software and compared to samples from aged matched control specimens.

Hemodynamic analysis, transverse aortic constriction and echocardiography.

Hemodynamic measurements were obtained on age matched 5 week old mice (n=8-10 in each group)[4]. Animals were anesthetized via intraperitoneal injection of 100 mg/kg ketamine and 5 mg/kg xylazine and placed on a warming pad. Heart rate and temperature were continuously monitored. Following anesthetization and intubation, the right carotid artery was exposed. A 1.4 French Millar catheter (Millar Instruments) was inserted and advanced until a left ventricular pressure tracing was visualized. The catheter was adjusted so that no catheter trapping was evident. The animals were recovered from the initial procedure and baseline pressure measurements were obtained. Sequential injections of graded doses of dobutamine were administered with at least a 5-minute recovery period between injections. Measurements were acquired with Hem Software (Notocord Systems). Heart rate and left ventricular pressure were recorded 150 seconds after the injections and averaged over a 10 second period. Maximum and minimum dP/dT were calculated during this 10 second period. The animals were given a lethal

dose of KCl to terminate the experiment.

Pressure overload hypertrophy was induced via transverse aortic constriction, using previously published techniques [5]. Animals were anesthetized and monitored as above. A midline cervical incision was made and the trachea was exposed. Animals were intubated with a 20 gauge blunt-tipped needle and then connected to a mechanical ventilator. The chest was entered at the left 2nd intercostal space. The thymus was deflected to expose the aorta. A constriction was made in the transverse aorta by tying a 7-0 silk suture over a 27-gauge needle. The pneumothorax was evacuated and the chest was closed. The animals were extubated approximately 20 minutes after the surgery and allowed to recover before being returned to their cages. Sham animals underwent an identical procedure without aortic constriction. Animals were monitored on a twice daily basis for survival.

For echocardiography mice were anesthetized with Avertin 2.5%, 14 μl/g intraperitoneally. The anterior chest was shaved and then mice were placed on a heating pad. An Apogee CX echocardiographic machine (ATL Interspec) incorporating a wide bandwidth transducer with dynamically focused symmetrical annular array technology that can be shifted to carrier frequencies of 9.0, 7.5, or 5.0 MHz was used for imaging. Small needle ECG leads (Grass Instruments) were placed through the skin on the right and left upper extremities and the left leg and connected to the machine for ECG timing. For two-dimensional and M-mode imaging, the 9.0-MHz frequency was used at a minimum depth setting of 3 cm and sector width of 40° to 50°. For pulsed-wave Doppler recordings, the minimum sample size (0.6 mm) was used and the pulse repetition frequency was 5 kHz. A standoff fashioned from polyethylene tubing (approximately 1.5 cm depth) was filled with centrifuged, warmed acoustic gel solution and used for imaging. Mice were oriented in the left lateral decubitus or supine position. For

determination of left ventricular parameters, short and long axis views were obtained. Echocardiographic measurements were averaged from at least 3 consecutive RR intervals determined from the LV M-mode tracings or from spectral Doppler tracings of the LV outflow tract. LV dimensions, wall thickness and parameters of contractility, such as LV fractional shortening (FS), and circumferential fiber shortening (vCf) were determined. The FS of the LV was expressed as a percentage as %FS=(LVDed-LVDes)/LVDed x 100. Using the aortic ET obtained from the Doppler tracing of the LV outflow tract, Vcf was determined as Vcf=(LVDed - LVDes)/(ETx LVDed). Images were captured digitally on a standard IBM PC using an ATI 128 Wonder video capture card (ATI) and then analyzed using Sigmascan (SPSS Software) that was calibrated to the scale recorded on each echocardiographic exam.

Histology and immunofluorescent microscopy. Sections (5 μm) of paraffin embedded heart were stained with hematoxylin and eosin or with Masson's Trichrome. Immunostaining of 5-7 μm cryosections of heart tissue was performed with antibodies to detect β1D integrin or talin [6] and analyzed with either a Nikon Diaphot or a Leitz confocal microscope equipped with epifluorescent optics. Percent fibrosis was quantified by determining the ratio of fibrotic areas to total ventricular tissue area visualized on digitally acquired images of left ventricular histological sections utilizing Sigmascan™ software (SPSS Software).

Electron microscopy. For thin-section electron microscopy tissue was perfusion fixed in glutaraldehyde followed by OsO_4. The heart was cut into pieces < 2mm in diameter, dehydrated in graded concentrations of ethanol, and embedded in epoxy resin. Ultra-thin sectioning was performed, sections were mounted on naked copper grids, post-stained with lead citrate and imaged with a JEOL 100 CX electron microscope[7].

REFERENCES

1. Chui D, Oh-Eda M, Liao YF, Panneerselvam K, Lal A, Marek KW, Freeze HH, Moremen KW, Fukuda MN, Marth JD. Alpha-mannosidase-II deficiency results in dyserythropoiesis and unveils an alternate pathway in oligosaccharide biosynthesis. *Cell.* 1997;90:157-167.

2. Joyner AL. Gene targeting: a practical approach. 1993. IRL Press at Oxford University Press, Oxford.

3. Gu H, Zou YR, Rajewsky K. Independent control of immunoglobulin switch recombination at individual switch regions evidenced through Cre-loxP-mediated gene targeting. *Cell.* 1993;73:1155-1164.

4. Rockman HA, Hamilton RA, Jones LR, Milano CA, Mao L, Lefkowitz RJ. Enhanced myocardial relaxation in vivo in transgenic mice overexpressing the beta2-adrenergic receptor is associated with reduced phospholamban protein. *J Clin Invest.* 1996;97:1618-1623.

5. Rockman HA, Ross RS, Harris AN, Knowlton KU, Steinhelper ME, Field LJ, Ross JJ, Chien KR. Segregation of atrial-specific and inducible expression of an atrial natriuretic factor transgene in an in vivo murine model of cardiac hypertrophy. *Proc Natl Acad Sci U S A.* 1991;88:8277-8281.

6. Keller RS, Shai SY, Babbitt CJ, Pham CG, Solaro RJ, Valencik ML, Loftus JC, Ross RS. Disruption of Integrin Function in the Murine Myocardium Leads to Perinatal Lethality, Fibrosis, and Abnormal Cardiac Performance. *Am J Pathol.* 2001;158:1079-1090.

7. Frank JS, Brady AJ, Farnsworth S, Mottino G. Ultrastructure and function of isolated myocytes after calcium depletion and repletion. *Am J Physiol.* 1986;250:H265-H275.

Legends for Supplementary Figures

Supplementary Figure 1 – Diagrammatic production of the β1 integrin null allele

Panel A – Partial restriction map of the wild-type β1 integrin gene. Exons 2 – 5 are shown as blue rectangles. The translational start site (ATG) is found in exon 2. Regions of the gene used as Southern blot probes for detecting appropriate gene-targeting are depicted as red boxes. B = BamHI, RV=EcoRV, RI=EcoRI.

Panel B – Diagrammatic representation of the β1 integrin gene targeting construct. Plasmid sequences are shown as green rectangles. N=NotI, RV=EcoRV, RI=EcoRI, B=BamHI, pGKNeo= phosphoglycerate kinase--bacterial neomycin, HSV-TK=herpes simplex virus thymidine kinase gene.

Panel C – Diagram of the β1 integrin gene following successful gene targeting with incorporation of loxP sites and retention of neomycin (Neo) and thymidine kinase (tk) selectable marker genes.

Panel D - Diagram of the targeted β1 integrin gene (from panel C above) following successful excision of the selectable marker genes by transient transfection of Cre-recombinase into the targeted embryonic stem cells. This was the structure of the gene found in the mice produced from the targeted ES cells.

Panel E – Diagram of the β1 integrin gene (shown in panel D) following Cre-mediated excision of exons 2 and 3. This result occurred specifically in cardiac myocytes following Cre-recombinase expression in these cells.

Supplementary Figure 2 – Analyses of successful gene targeting of the β1 integrin gene in embryonic stem cells.

Panel A and B – Southern blot analyses of representative embryonic stem cell clones following electroporation with the β1KO targeting vector.

Panel A - Genomic DNA from targeted embryonic stem cell clones was cut with EcoRI, blotted and detected with a β1 integrin gene exon 5 probe. This probe is located outside of the β1 integrin gene sequence incorporated into the targeting construct. As shown in Supplementary figure 1, the 12.5 kb band is detected in the wild-type allele, while the novel 9.4 kb band is detected in the appropriately targeted allele. Clones such as shown in lane 6, with equal intensity of the 12.5 and 9.4 kb bands, were used for further work.

Panel B - Genomic DNA from targeted embryonic stem cell clones was cut with BamHI, blotted and detected with a β1 integrin gene probe from intron 1. The 10.9 kb band is detected from the wild-type allele while the 5.1 kb band is only detected in the targeted allele. Clones such as shown in lane 2, were used for further work.

Panel C – Diagram of the Wild-type β1 integrin gene, the appropriately targeted allele and the targeted allele following excision of the selectable markers. Regions of primer sequences used in the PCR (Panel D, below) are shown in green (PR2 and PR3). LoxP sites are shown as purple triangles, exons as blue rectangles.

Panel D – Polymerase chain reaction products generated from β1 integrin gene targeted embryonic stem cell DNA, following transient Cre-recombinase expression. Genomic DNA was derived from ES cell clones which had been previously shown by Southern blot analyses to

be correctly targeted in the β1 integrin gene locus, and was subsequently transiently transfected with pMC-Cre. PCR was performed on this template DNA using primers 2 and 3 (PR2 and PR3 shown in panel C above). This primer set yielded a 167 bp band in the wild type β1 integrin gene allele and a 245 bp band in the β1 integrin gene allele which was both targeted correctly and also had production of a type-II deletion following transient Cre-mediated excision of the selectable marker genes pGKNeo and HSV-Tk. (As diagrammed in panel C above.) The primer set would yield a 3.5 kb PCR band from the β1 integrin gene allele which was targeted but still retained the selectable markers, and thus would not be detected on this representative agarose gel.

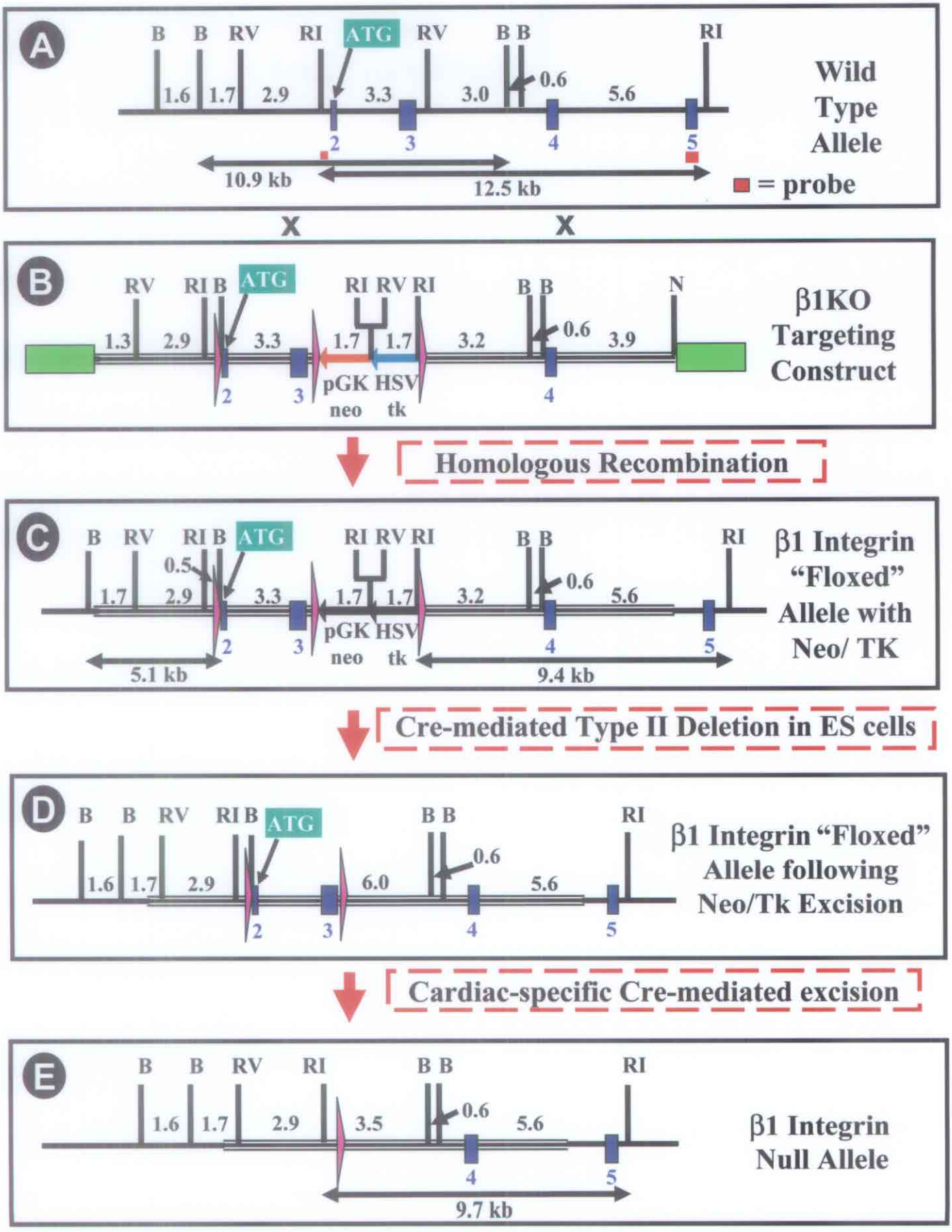

Supplementary Figure 1

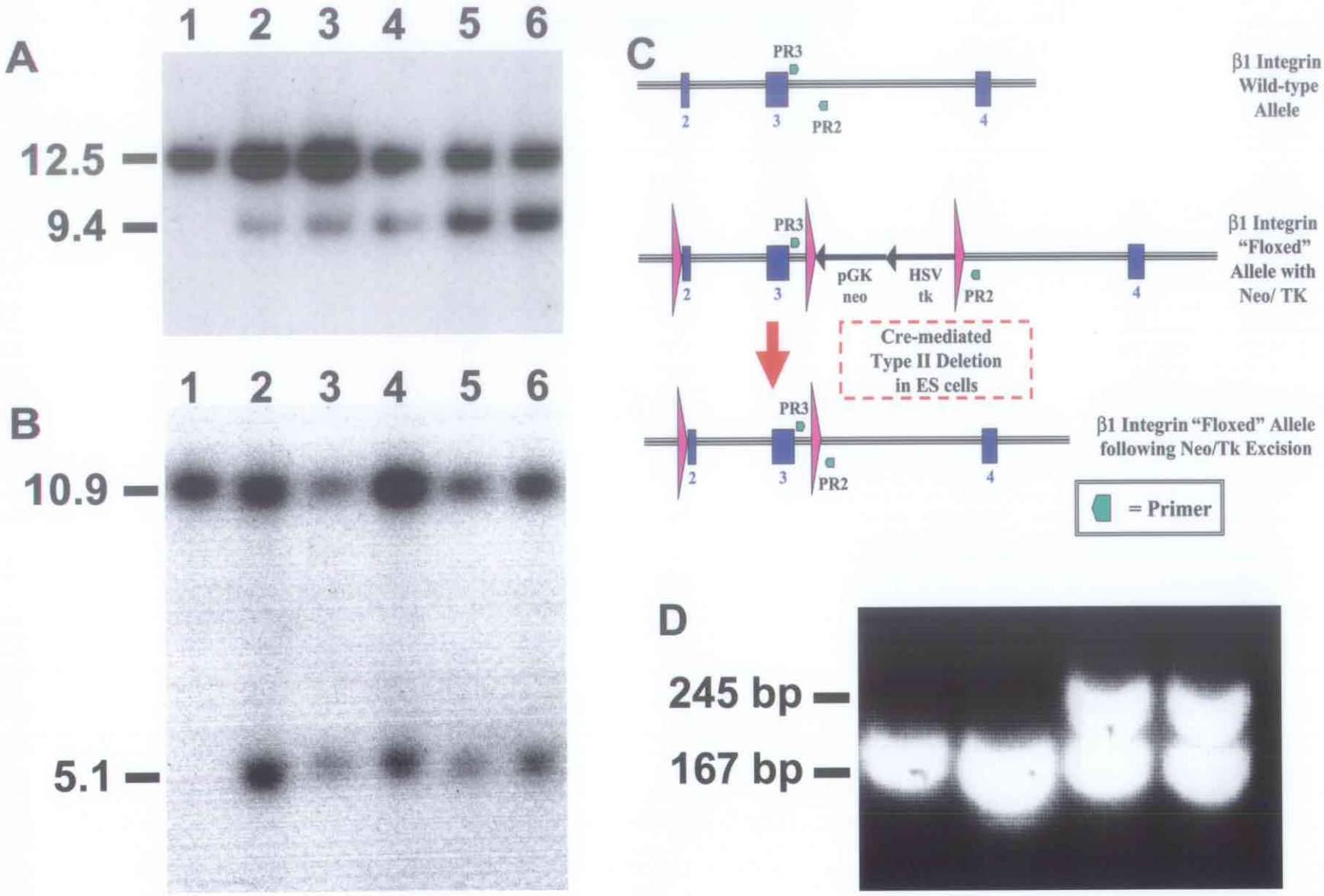

Supplementary Figure 2